ELSEVIER

Ceramics International 25 (1999) 717–721

CERAMICS
INTERNATIONAL

Densification of nanosized amorphous and crystalline silicon nitride powders

János Szépvölgyi*, Ilona Mohai

Research Laboratory of Materials and Environmental Chemistry, Chemical Research Center, Hungarian Academy of Science,
H-1025 Budapest, Pusztaszeri út 59–67, Hungary

Received 15 October 1998; received in revised form 26 October 1998; accepted 10 December 1998

Abstract

The hot-pressing behavior of two amorphous and three crystalline silicon nitride powders, including both experimental and commercial samples has been investigated in the presence of MgO-Y_2O_3 sintering aid. The powders were characterized in terms of bulk and surface chemistry, phase composition and morphology. The sintering behavior was assessed on the basis of green and final densities, weight loss on densification and chemical and phase compositions of the dense material. © 1999 Elsevier Science Ltd and Techna S.r.l. All rights reserved.

Keywords: A. Hot pressing; D. Si_3N_4; Amorphous; Crystalline; XPS (ESCA)

1. Introduction

Dense silicon nitride-based ceramics are usually produced by sintering sub-micrometer silicon nitride powders of controlled oxygen content. Silicon nitride is characterized by covalent bonds and very low atomic self-diffusion. Thus, liquid-forming sintering aids, such as Y_2O_3, MgO and Al_2O_3 added singularly or in combination, must be used to achieve theoretical density.

Liquid-phase sintering of silicon nitride is conventionally considered to be a multi-stage process: (i) particle rearrangement aided by the lubricant action of the liquid, (ii) dissolution and crystallization of very fine grains and (iii) dissolution and re-crystallization of coarser grains. Rate control in the second and third stages is either an interface dissolution or crystallization, or diffusion of "Si_3N_4" through the liquid from regions of high chemical potential to regions of low potential [1–3].

With low viscosity liquids, based for example on MgO, surface reactions appear to be rate controlling [4], although in hot-pressing diffusion has been assumed to be rate controlling [2]. With highly viscous liquids, based for example on Y_2O_3, diffusion is usually [5], however, not always [6] considered as rate controlling.

Analyses based on the classical Kingery model of liquid-phase sintering are made by measuring shrinkage as a function of time. However, complications arise because the reference zero time appropriate for stage (ii) data is uncertain, and the stages may also overlap. Furthermore, there is the added uncertainty about the influences of initial particle rearrangement, and subsequent grain growth on densification rate. Nonetheless, it is useful to be able to rank powder quality by measuring densification rate under standardized sintering conditions.

It should be mentioned, however, that microstructure is property controlling, and a rapid densification does not necessarily yield the optimum properties of the silicon nitride ceramics, ultimately. An appropriate sintering schedule, especially in the final stage, is important for microstructure development.

Dense silicon nitride ceramics require high purity, fine powders of narrow size distribution [7]. With respect to sintering activity, amorphous Si_3N_4 of high surface energy offers considerable theoretical advantages [8], because of the availability of a high amount of crystallization energy. In this paper we report a comparative study on the densification behavior of two amorphous and three crystalline silicon nitride powders before, during and after hot pressing.

---

* Corresponding author. Tel.: +36-1325-7896; fax: +36-1325-7892.
E-mail address: szepvol@cric.chemres.hu (J. Szépvölgyi).

PII: S0272-8842(99)00007-3

2. Experimental

2.1. Characteristics of powders

The grades and characteristics of powders selected for the investigations are presented in Table 1. Laboratory samples *SNP-1*, *SNP-2* and *SNP-2C* were prepared by the vapor-phase reaction of $SiCl_4$ and NH_3 in a RF thermal plasma reactor [9]. Methods and conditions of analysis are referred in a former work [10].

The *SNP-1* and *SNP-2* powders prepared by vapor-phase synthesis were predominantly amorphous, while the others were mostly crystalline. α-Si_3N_4 was the major crystalline phase in all samples, as shown by the α/β ratios.

The two amorphous powders had very high specific surface areas and small mean particle sizes. Crystallization of the *SNP-2* powder resulted in a considerable decrease of specific surface area. The silicon dioxide or "oxygen" content of the powder is an important factor, because silicon dioxide provides the silicate liquid during sintering. Oxygen may be introduced into the powder either during synthesis or by post-fabrication hydrolysis and oxidation. Therefore, both the oxygen content, and the distribution of the oxygen between the bulk of a particle and its surface are likely to be important for silicate generation rate and thus sintering rate. The surface chemistry of the powders was studied by X-ray photoelectron spectroscopy (XPS), as it was described previously [11].

In all powders a remarkable surface oxygen enrichment was detected. Both the total and the surface oxygen contents of the powders increased with increasing specific surface area (Fig. 1). The surface oxygen also increased with the total oxygen content of powders (Fig. 2). The chemical states of surface silicon in *SNP-1* were determined from the XPS investigations by deconvoluting the Si2p signal envelope. It was found that the composition of the surface oxide layer corresponds to an intermediate state between silica and silicon oxy-nitride. It was also established that in the amorphous experimental powders (*SNP-1* and *SNP-2*), and in the commercial powder *SN E-10*, all the oxygen is concentrated near the surface, as a consequence of post-fabrication oxidation and hydrolysis in the ambient atmosphere [10].

2.2. Mixing of sintering aids

The densification behavior was assessed by hot-pressing powders containing either a 10 m% (*SNP-1D*, *LC12-SXD* and *SN E-10D*) or a 5 m% (*SNP-2D* and *SNP-2CD*) equimolar mixture of MgO and Y_2O_3. The latter samples contained less dopant because of the relatively high oxygen content of powders.

2.3. Hot-pressing

Hot pressing was carried out at 1650°C and 10 MPa, in a 25 mm graphite die internally coated with boron nitride. The pressure was applied from the beginning of the hot-pressing test. The hot-pressed materials were analyzed for bulk nitrogen, oxygen and silicon. Surface (XPS) analyses were made on freshly broken surfaces. Phase composition was determined by XRD.

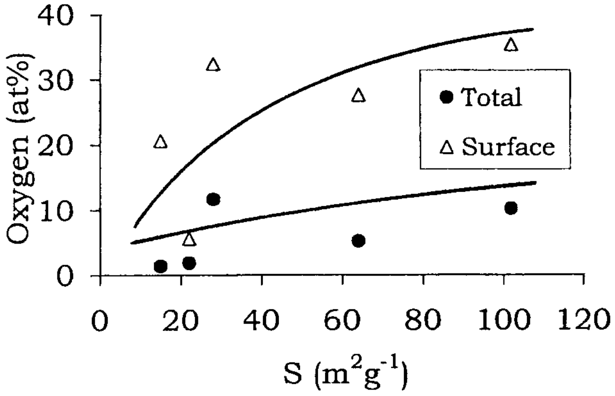

Fig. 1. Oxygen content as a function of specific surface area.

Table 1
Characteristics of silicon nitride powders selected for investigations

No[a]	N	O	Si	C	ΣMe	Amor. (%)	α/β Si_3N_4	S (m^2 g^{-1})	D (nm)
	(at%)								
SNP-1	52.7	5.2	42.0	0.08	0.02	> 80	4	64	30
SNP-2	47.6	10.3	42.0	0.10	0.04	> 80	4	102	18
SNP-2C	48.8	11.7	39.4	0.10	0.02	< 10	8	28	67
LC12-SX	55.1	1.9	42.7	0.28	0.06	< 5	30	22	86
SN E-10	54.7	1.3	43.8	0.16	0.02	< 5	48	15	126

[a] *SNP-1* experimental powder collected from the plasma torch; *SNP-2* experimental powder collected from the dust separation unit connected to the torch; *SNP-2C* crystallized SNP-2 (0.1 MPa N_2, 1450°C, 6 h); *LC12-SX* commercial powder produced by nitridation of silicon (Starck Co.); *SN E-10* commercial powder produced by the diimide route (UBE Co.)

3. Results and discussion

Conditions and results of hot pressing are shown in Table 2. Two sets of conditions were used: (i) hot-pressing was stopped after 20 s to study the very early stages of densification and (ii) the powders were hot-pressed until no more densification was detected (2–6 ks). The fastest powder to densify was *SNP-2CD* (1.8 ks). The amorphous, high specific surface area *SNP-2D* powder had the longest densification time (5.4 ks), probably due to the low green density.

Both green and final relative densities of compacts prepared from experimental powders *SNP-1D*, *SNP-2D* and *SNP-2CD* were lower than those obtained with the two commercial powders (Table 2), as expected.

The relative densities decreased with increasing specific surface area of blended powders (Fig. 3). There was no correlation between powder phase composition and green and final densities. Final relative densities are shown as functions of total and surface oxygen contents of blended powders in Fig. 4. The importance of oxygen is clear.

Small mass losses ($\Delta m/m_0$) were measured during the heating of powders *SNP-1D* and *SNP-2CD* to the hot-pressing temperature (Table 2, *P12* and *P2C2*). A greater weight loss was detected at the high surface area *SNP-2D* powder. The final weight loss increased with increasing total oxygen content and specific surface area, respectively, except for the crystalline *SNP-2CD* powder.

The following chemical reactions may provide mass losses on sintering:

$$Si_3N_4(s) = 3\ Si(l) + 2\ N_2(g) \quad (1)$$

$$2\ Si(l) + O_2(g) = 2\ SiO(g) \quad (2)$$

$$2\ Si_3N_4(s) + 1.5\ O_2(g) = 3\ Si_2N_2O(s) + N_2(g) \quad (3)$$

$$2\ Si_2N_2O(s) = Si_3N_4(s) + SiO(g) + 0.5\ O_2(g) \quad (4)$$

$$Si_2N_2O(s) + 1.5\ O_2(g) = 2\ SiO_2(s, l) + N_2(g) \quad (5)$$

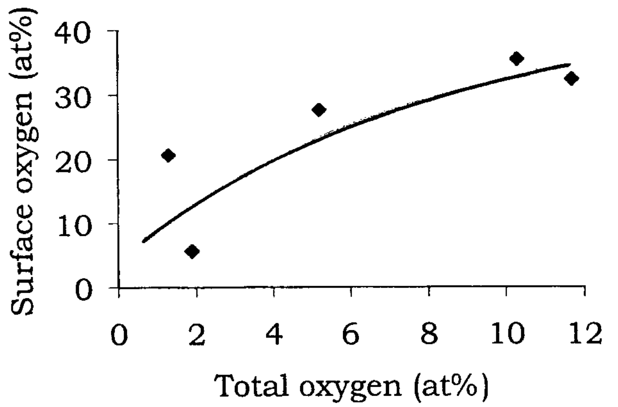

Fig. 2. Surface oxygen content as a function of total oxygen content.

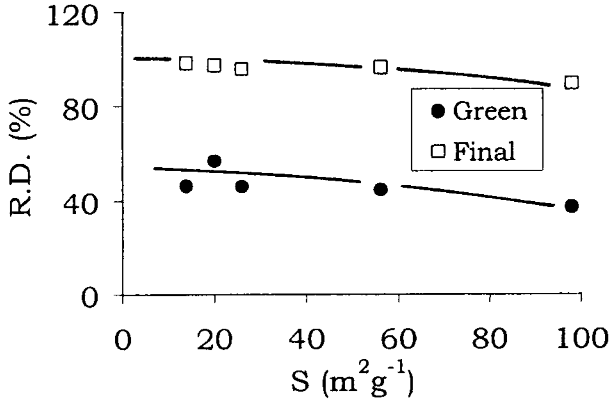

Fig. 3. Relative density as a function of specific surface area of blended powder.

Table 2
Conditions and results of hot pressing[a]

Blended powder	HP material	*t* (s)	$\Delta m/m_0$ (%)	D_{th} (g cm^{-3})	Green R.D. (%)	Final R.D. (%)
SNP-1D	*P12*	20	0.3	3.20	45.3	52.5
SNP-1D	*P11*	2400[b]	7.3	3.20	45.0	96.6
SNP-2D	*P22*	20	5.6	3.15	37.7	42.5
SNP-2D	*P21*	5400[b]	9.6	3.15	37.7	89.8
SNP-2CD	*P2C2*	20	0.1	3.13	46.3	53.1
SNP-2CD	*P2C1*	1800[b]	1.9	3.13	46.3	95.8
LC12-SXD	*P31*	3600[b]	5.1	3.25	56.9	97.5
SN E-10D	*P41*	2400[b]	5.2	3.25	46.5	98.5

[a] *t*, hot-pressing time, $\Delta m/m_0$ mass loss on hot-pressing, D_{th} theoretical density, R.D. relative density.
[b] Full densification.

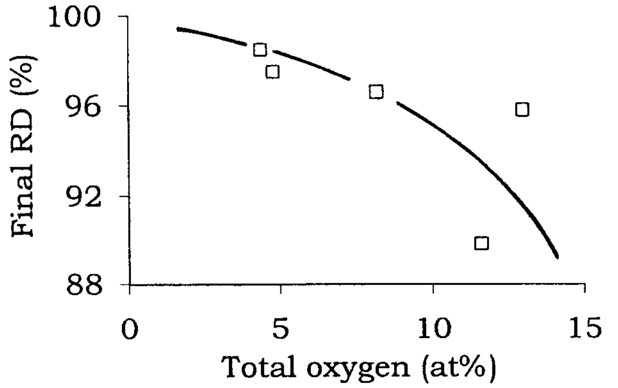

Fig. 4. Final relative density as a function of total oxygen content of powder.

Table 3
Chemical and phase compositions of hot pressed materials

HP material	Chemical composition (at%)			Phase composition (mol%)		
	N	O	Si	α-Si_3N_4	β-Si_3N_4	Si_2N_2O
P12	44.7	9.6	37.9	27	15	45
P11	46.1	8.7	37.2	4	49	34
P22	43.0	13.3	39.8	–	29	65
P21	43.7	12.8	39.3	–	31	62
P2C2	45.7	12.5	37.2	21	8	63
P2C1	46.6	12.0	36.7	8	27	58

However, there is no change in the mass when Si_3N_4 and SiO_2 react with each other:

$$Si_3N_4(s) + SiO_2(s, l) = 2\ Si_2N_2O(s) \qquad (6)$$

Decomposition of Si_3N_4 becomes increasingly important above 1500°C. Because the heating of the powder from 1500 to 1650°C took 540 s it is likely that Si_3N_4 partly decomposes soon at this stage.

Chemical compositions of dense materials (Table 3) suggest that prior to hot pressing the dominant reactions are Eqs. (1), (3) and (6). During hot-pressing reactions Eqs. (2), (4) and (5) are likely to take place.

The amorphous powders had varying degrees of crystallization and α/β ratio. However, these powders contained more than 90% crystalline phase at the very beginning of hot-pressing (Table 3), indicating that solution and crystallization occurred at temperatures lower than 1650°C. Si_2N_2O was the dominant crystalline phase in these samples, and Y-containing crystalline phases were absent. This is in agreement with Ekström et al. [12], who observed that the intergranular glassy phase contained all the yttrium. The fraction of Si_2N_2O decreased, and that of β-Si_3N_4 increased during hot pressing. In addition, there was a significant α-Si_3N_4 to β-Si_3N_4 transformation. Hot pressing of *LC12-SXD* and *SN E-10D* powders gave materials containing 64 and 53 mol% β-Si_3N_4, respectively [13].

XPS measurements of the fractured surfaces of dense materials revealed a surface enrichment of N and Mg, and a reduction of O against Si, as compared to the doped powder. No yttrium was detected on the fractured surface, indicating an inward segregation of yttrium [10].

4. Conclusions

Nanosize silicon nitride powders produced by different synthesis routes differ considerably in their bulk and surface compositions, crystalline phase content and morphology. The oxygen content of powders prepared in the thermal plasma is concentrated near to the particle surface, similarly to the crystalline powder produced by diimide decomposition. Post-synthesis oxidation and hydrolysis are likely to occur in these powders.

Nanosize silicon nitride particles dissolve very rapidly in the liquid phase during hot pressing. Dissolution most probably starts before the hot-pressing temperature is reached. Therefore, it actually does not matter, whether the oxygen is on the surface, or in the bulk of particles. Dissolution is followed by a very rapid precipitation of Si_3N_4 and Si_2N_2O. The amorphous powders contain more than 90% crystalline phase at the very beginning of hot pressing. The higher oxygen content of the powders, the more Si_2N_2O will form. At longer hot pressing times α-Si_3N_4 and Si_2N_2O transform to β-Si_3N_4.

Oxygen content and specific surface area of powders are likely to be important properties for controlling the densification and microstructure. Microstructural development of materials produced with nanosize, plasmathermal powders does not seem to depend on the presence of α-Si_3N_4.

Acknowledgements

The authors are grateful for the financial support of the OTKA fund No. T16175.

References

[1] W.D. Kingery, Densification during sintering in the presence of a liquid phase, J. Appl. Phys. 30 (1959) 301–306.

[2] R.J. Brook, E. Gilbart, N.J. Shaw, U. Eisele, Solid solution additives and the sintering of ceramics, Powder Metall. 28 (1985) 105–107.

[3] R.M. German, S. Farooq, C.M. Kipphut, Kinetics of liquid phase sintering, Mat. Sci. Eng. A. 105–106 (1988) 215–224.

[4] F. Cambier, A. Leriche, E. Gilbart, R. J. Brook, F. L. Riley, Silicon-nitride: relations between powder characteristics and sinterability, in: The Physics and Chemistry of Carbides, Nitrides and Borides, NATO ASI Series E: Applied Sciences, Vol. 185, Kluwer Academic Press, London, 1989, pp. 13–28.

[5] A. Bellosi, C. Galassi, D.D. Fabbriche, Sintering characteristics of Si_3N_4 powders, High temperatures–High Pressures 20 (1988) 335–343.

[6] O. Abe, Sintering process of yttria-added silicon nitride (Si_3N_4), J. Mater. Sci 25 (1990) 3641–3648.

[7] G. Ziegler, H. Heinrich, G. Wötting, Relationships between processing, microstructure and properties of dense and reaction-bonded silicon nitride, J. Mater. Sci. 22 (1987) 3041–3086.

[8] M. Mitomo, Thermodynamics, phase relations and sintering aids of silicon nitride, in: Somiya, S., Mitomo, M., Yoshimura, M. (Eds.), Silicon Nitride–1, Elsevier, London, 1990, pp. 1–12.

[9] J. Szépvölgyi, I. Mohai-Tóth, Experimental investigation into the synthesis of silicon nitride powder in an RF thermal plasma reactor using a factorial design approach, J. Mater. Chem. 5 (1995) 1227–1232.

[10] J. Szépvölgyi, I. Mohai, Comparative hot-pressing study of amorphous and crystalline silicon nitride powders, in: Engineering Ceramics 96 (NATO ASI Series), Kluwer Academic Publishers, Dordrecht, The Netherlands, 1997, pp. 89–107.

[11] I. Bertóti, G. Varsányi, G. Mink, T. Székely, J. Vaivads, T. Millers, J. Grabis, XPS characterization of ultrafine Si_3N_4 powders, Surf. Interface Anal. 12 (1988) 527–530.

[12] T. Ekström, M, Holmström, P.O. Olson, Yttria doped Si_2N_2O, in: Proc. 4th Int. Symp. Ceramic Materials and Components for Engines, Elsevier, London, 1992, pp. 432–439.

[13] J. Szépvölgyi, I. Tóth, I. Bertóti, E. Gilbart, F.L. Riley, M. Patel, Comparative sintering studies on non-conventional and commercial silicon nitride powders, J. Mater. Chem. 3 (1993) 279–286.